

Exact Calculation of $ff \rightarrow ffWW$ for the Charged-Current Sector and Comparison with the Effective- W Approximation

J. F. Gunion, J. Kalinowski,^(a) and A. Tofighi-Niaki

Department of Physics, University of California at Davis, Davis, California 95616

(Received 2 September 1986)

We have computed the complete set of amplitudes for fermion+fermion into fermion+fermion+ W^+ + W^- for all possible fermion types. We use these results to analyze the phenomenology of the WW scattering sector and to compare to the effective- W approximation.

PACS numbers: 13.85.Qk, 12.15.Ji, 13.10.+q, 14.80.Er

The most important untested predictions of the standard $SU(2)_L \otimes U(1)$ model are those for gauge-boson scattering, which are, in particular, sensitive to the Higgs resonance and exchange diagrams. Results for on-shell WW scattering have appeared in the literature.¹ However, these amplitudes are not directly relevant in the actual experimental situation. In order to test the on-shell forms, it is necessary to rely on the effective- W approximation² in which distributions for W 's inside colliding e^+e^- or pp beams are folded together with the on-shell amplitudes, much as in the conventional two-photon approximation.³ The validity of the effective- W approximation has been examined in the reactions $W^+W^- \rightarrow H^4$ (where the H is treated as stable) and $qg \rightarrow q'UD^5$ (where U and D are the quarks of a new generation). In both cases, the approximation was valid for total-cross-section computations at the level of 20%. However, the correctness of this approach in the context of WW scattering remains an open question which we shall address here. In addition, the effective- W approximation cannot be reliably used to assess the impact of possible triggers on the secondary spectator quarks present, along with the W 's, in the final state. Such triggers may prove to be critical in isolating the interesting aspects of WW scattering (in particular, the Higgs component) from backgrounds at the Superconducting Super Collider.⁶

To address the above issues we have computed the complete gauge-invariant set of amplitudes contributing to an arbitrary $ff \rightarrow ffW^+W^-$ process, using the massless spinor techniques of Gunion and Kunszt.⁷ In this technique the final-state W 's are automatically decayed to massless fermions, so that the amplitudes include full spin-density-matrix decay correlations for all final-state products.

In the present paper we shall focus exclusively on issues relevant to the charged-current reactions to which WW scattering diagrams contribute, and leave more general phenomenological considerations to a later work. The charged-current reactions have the advantage over test cases which include $ZZ \rightarrow W^+W^-$ scattering subprocesses, such as $uu \rightarrow ddW^+W^-$, of containing no two-photon scattering contributions; these latter contributions provide a potentially difficult background and

will be addressed elsewhere. For simplicity, we shall only present explicit numerical results for the quark scattering process

$$us \rightarrow dcW^+W^-. \quad (1)$$

Those for the $e^+e^- \rightarrow \bar{\nu}_\nu W^+W^-$ reaction are entirely analogous. For our quark-sector calculations we have set the Cabibbo angle to zero. There are only 35 contributing Feynman diagrams (counting Z , γ , and H exchanges separately) in both Feynman and unitary gauge. In addition, there is only one contributing helicity amplitude, namely that for which all outgoing fermions have negative helicity. Of course, the above statements apply only to the purely electroweak scattering contributions. In the quark reaction (1) there is an additional set of diagrams arising from gluon-exchange scattering of the quarks, accompanied by W bremsstrahlung. Such processes will be considered separately towards the end of this paper.

In order to probe the accuracy of the effective- W approximation with maximum sensitivity, we will focus on results at the subprocess level for reaction (1). For simplicity we will take $E_{c.m.} \equiv \sqrt{s_{us}} = 1$ TeV and consider only $m_H = 500$ GeV or $m_H = \infty$. Our results are illustrative of those for other energies and Higgs-boson masses. We begin by presenting the m_{WW} , W -pair mass, spectrum for both the exact and effective- W calculations in Fig. 1. In order to make a comparison, it is necessary to impose a cut in the effective- W computation which avoids the t -channel singularity of on-shell WW scattering deriving from photon exchange. We have chosen to impose the restriction

$$\theta_{WW}^* > \theta_{\min} \quad (2)$$

upon the WW center-of-mass scattering angle. The exact calculation is free of this singularity; however, for comparison the cut (2) is also imposed. Figure 1 shows that the effective- W spectra normalization is very sensitive to this cut, while that of the exact calculation is much less so. For instance, at $\theta_{\min} = 60^\circ$ the nonresonant effective- W continuum has fallen by a factor of roughly 19 from its $\theta_{\min} = 10^\circ$ level, whereas the exact calculation continuum background varies by a factor of order 1.5 to 2, depending on m_{WW} value. In contrast, the excess of

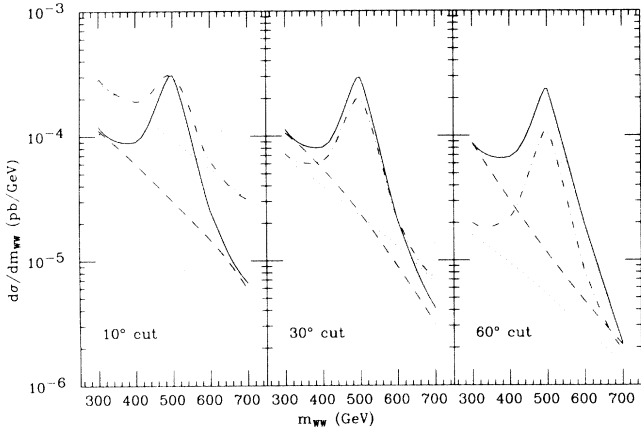


FIG. 1. W -pair mass spectra $d\sigma/dm_{WW}$ for Reaction (1) at $E_{c.m.}=1$ TeV. Spectra are shown for (i) exact calculation, $m_H=500$ GeV (solid curve); (ii) exact calculation, $m_H=\infty$ (dashed curve); (iii) effective- W calculation, $m_H=500$ GeV (dash-dotted curve); and (iv) effective- W calculation, $m_H=\infty$ (dotted curve). We have chosen different cuts, as described in the text, on the WW center-of-mass scattering angle.

the $m_H=500$ GeV peak over the $m_H=\infty$ continuum is very comparable in the two calculations, in agreement with Ref. 4. In the exact calculation it decreases by about 15% in going from $\theta_{min}=10^\circ$ to $\theta_{min}=60^\circ$; in the effective- W calculation this excess decreases by about a factor of 2 over the same range. Thus we conclude that the effective- W approach yields a good approximation to

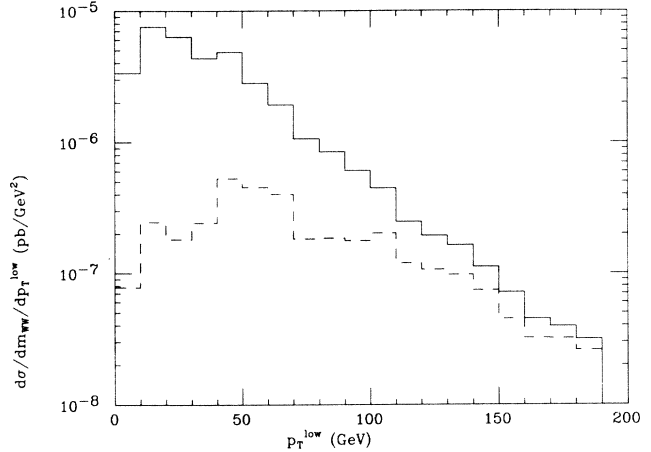


FIG. 2. Spectator transverse momentum distribution $d\sigma/dm_{WW} dp_T^{WW}$ from Reaction (1) for $E_{c.m.}=1$ TeV; $m_{WW}=500$ GeV. Solid histogram, $m_H=500$ GeV; dashed histogram, $m_H=\infty$.

the Higgs signal, but is generally unreliable for computing the background from the general subprocess set.

We turn now to various phenomenological features of the exact calculation. The longitudinal polarization of a final-state W is revealed in two ways: (a) by a $\sin^2\theta^*$ vs $1+\cos^2\theta^*$ decay distribution for the $f\bar{f}'$ from the W decay in its rest frame; and (b) by correlations between the transverse momenta of the decay products from the W . Only (b) can be used for hadronic $f\bar{f}'$ decay modes due

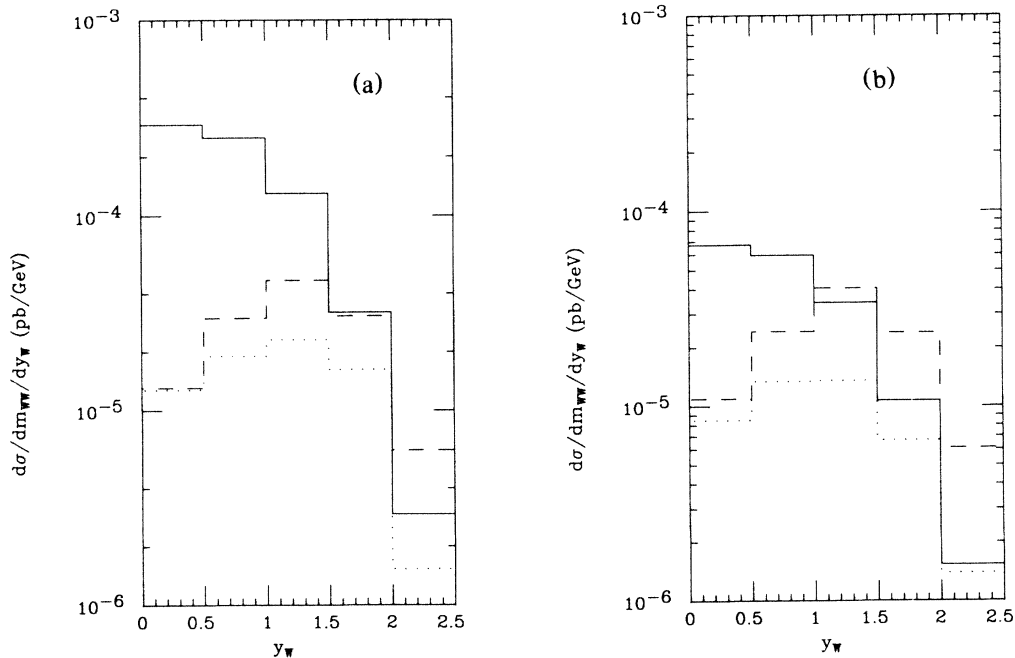


FIG. 3. W rapidity distribution $d\sigma/dm_{WW} dy_W$ at $E_{c.m.}=1$ TeV and $m_{WW}=500$ GeV, for the purely electroweak subprocesses (solid histogram, $m_H=500$ GeV; dotted histogram, $m_H=\infty$), compared with that for the gluon-exchange mechanism (dashed histogram). (a) No p_T^{WW} cut; (b) $p_T^{WW} > 50$ GeV.

to backgrounds from mixed strong-electroweak processes.⁸ Both have been explored in an earlier work,⁹ in the effective- W approximation. We have reexamined these longitudinal W decay signatures in the exact calculation, which, in particular, includes transverse momentum for the WW system, and we confirm that both signatures for the longitudinal W 's produced by Higgs-boson decay emerge on resonance, $m_{WW} = m_H = 500$ GeV.

The totally new feature of the present exact calculation is the ability to examine the behavior of the spectator final-state quarks that are inevitably present in process (1). In particular, it has been suggested in Ref. 6 that triggering on one or both of the spectator quarks at significant transverse momentum could substantially reduce backgrounds to the Higgs-boson signal, coming both from the $q\bar{q} \rightarrow W^+W^-$ continuum subprocesses and from jjW backgrounds. The background processes tend to have spectator jets which are dominantly at low transverse momentum. To examine the nature of the spectator jet distribution from reaction (1), which contains both a Higgs-boson signal and background continuum processes, we have chosen to look at the spectator jet with smallest transverse momentum, p_T^{low} , in the us center of mass. Single spectator distributions are quite similar to those we give. In Fig. 2 we present the p_T^{low} spectra for reaction (1). It is immediately apparent that the Higgs-boson signal has a steeper spectrum in p_T^{low} than do the continuum processes also contributing to (1). Thus a

trigger requiring some minimum value of p_T^{low} , while decreasing some backgrounds, will tend to increase the importance of the continuum background arising from reactions that must be included, along with the WW fusion mechanism for Higgs production, as part of a complete gauge-invariant set. For instance, before imposing any p_T^{low} cut, the ratio R of signal over this intrinsic background at $m_{WW} = 500$ GeV is close to $R = 10$. After imposing a cut of $p_T^{\text{low}} > 80$ GeV this ratio becomes $R = 2.5$.

We have also obtained results for all the above distributions at $E_{\text{c.m.}} = 3$ TeV, and for $m_H = 500$ GeV and $m_H = \infty$. All qualitative conclusions are the same. However, the extended energy range does allow investigation of much higher m_{WW} values. The most noteworthy new feature, at $m_{WW} = 1.5$ TeV for instance, is the increase in the fraction of longitudinal W 's in the final state, as revealed by the decay angular distributions in $\cos\theta^*$ and transverse-momentum correlations.

Let us next turn to a new background, namely the mixed strong-electroweak process contributing to reaction (1), in which a gluon is exchanged between the scattering quarks and W 's are emitted from either the initial- or final-state quarks. We shall see that a rapidity cut on the W 's is absolutely vital in eliminating this background. This is illustrated in Fig. 3, from which it is clear that the gluon-exchange diagrams contribute primarily to large values of y_W . From Fig. 3(a) it is apparent that a rapidity cut at $y_W = 1.5$ would be adequate

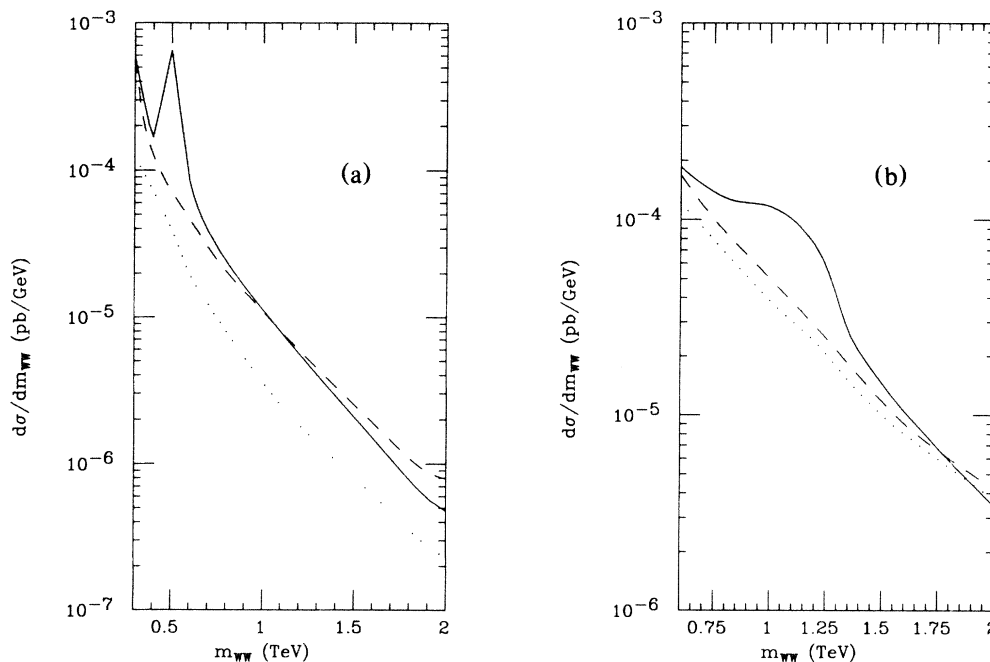


FIG. 4. W -pair mass spectra $d\sigma/dm_{WW}$ for pp collisions at $\sqrt{s} = 40$ TeV, with only the process $us \rightarrow dc$ included. (a) $|y_W| < 1.5$. Solid curve, purely electroweak processes, $m_H = 500$ GeV; dashed curve, same but $m_H = \infty$; dotted curve, gluon-exchange process. (b) $|y_W| < 2.5$. Solid curve, as in (a) but $m_H = 1$ TeV; dashed and dotted curves, as in (a). We have assumed that one W decays hadronically and the other leptonically, and thus have constrained both jets and the charged lepton from these decays to have $|y| < 4$.

if no p_T^{low} cut is required. On the other hand, the gluon-exchange and continuum-type background both increase relative to the Higgs-boson signal if $p_T^{\text{low}} > 50$ GeV is required [Fig. 3(b)] and a cut of $y_W < 1$ would be necessary. Thus the imposition of spectator-quark cuts in order to reduce backgrounds from other WW continuum and jjW reactions must be done with care in order to avoid the backgrounds to the Higgs-boson signal intrinsically present in reactions of the type (1).

For the Superconducting Super Collider, predictions require folding the above subprocess level phenomenology with the proton's quark distribution functions. Many of the same qualitative conclusions survive. Here we confine ourselves to presenting the invariant m_{WW} mass distribution, at $\sqrt{s_{pp}} = 40$ TeV, both for the electroweak amplitudes and for the gluon-exchange amplitudes. Only the single subprocess (1) is incorporated, folded with u and s distribution functions. The Q^2 scale of the distribution functions is chosen at $Q = m_{WW}$. In the gluon-exchange diagrams the strong-coupling-constant scale is chosen to be the momentum transfer carried by the gluon. As anticipated from the subprocess level calculations, a W rapidity cut is very effective in reducing the level of the gluon-exchange background, while sacrificing only a modest reduction in the Higgs-resonance cross section. Comparing the two rapidity-cut cases of Fig. 4 we also see that a stronger W rapidity cut reduces substantially the high- m_{WW} tails of all cross sections.

In conclusion, the full amplitude calculations, incorporated in the results presented here, make unambiguous computations for W -pair production possible. The complete phenomenology, including the neutral as well as charged-current-sector subprocesses, is in progress. From the present results we can conclude that the characteristics of longitudinal W 's, both angular decay distributions and transverse-momentum correlations of their decay products, that are crucial to isolating a Higgs-boson signal are substantially the same in the complete calculation as in the effective- W calculation. In ad-

dition, it is apparent that the potentially dangerous gluon-exchange background does not, in fact, present a problem, if rapidity cuts on the W 's are imposed.

We would like to thank R. Cahn, S. Dawson, G. Kane, and S. Willenbrock for helpful conversations. In addition we are grateful to W. Repko for providing us with an effective- W program which could be adapted for these studies. This work was supported in part by the U.S. Department of Energy.

(a)On leave of absence from Warsaw University, Warsaw, Poland.

¹C. Duncan, G. Kane, and W. Repko, Nucl. Phys. **B272**, 517 (1986).

²M. Chanowitz and M. K. Gaillard, Phys. Lett. **142B**, 85 (1984); S. Dawson, Nucl. Phys. **B249**, 42 (1985); G. Kane, W. Repko, and W. Rolnick, Phys. Lett. **148B**, 367 (1984); M. Chanowitz and M. K. Gaillard, Nucl. Phys. **B261**, 379 (1985).

³See, for example, the classic review of V. M. Budnev, I. F. Ginzburg, G. V. Meledin, and V. G. Serbo, Phys. Rep. **15C**, 183 (1974).

⁴R. Cahn, Nucl. Phys. **B255**, 341 (1985), and **B262**, 744(E) (1985).

⁵S. Dawson and S. Willenbrock, Lawrence Berkeley Laboratory Report No. LBL-21914, 1986 (to be published); J. Lindfors, Laboratoire de Physique des Particules Report No. LAPP-TH-160, 1986 (to be published).

⁶R. Cahn, S. Ellis, R. Kleiss, and W. J. Stirling, Lawrence Berkeley Laboratory Report No. Print-86-031 (to be published), presented at the University of California at Los Angeles Workshop on Standard Model Physics at the Superconducting Super Collider.

⁷J. F. Gunion and Z. Kunszt, Phys. Lett. **161B**, 333 (1985). See also the related work of R. Kleiss and W. J. Stirling, Nucl. Phys. **B262**, 235 (1985).

⁸J. F. Gunion, Z. Kunszt, and M. Soldate, Phys. Lett. **163B**, 389 (1985), and **168B**, 427(E) (1986).

⁹J. F. Gunion and M. Soldate, Phys. Rev. D **34**, 826 (1986).